Regularization-independent study of renormalized nonperturbative quenched QED

Ayşe Kızılersü,* Tom Sizer,† and Anthony G. Williams‡
Special Research Centre for the Subatomic Structure of Matter and Department of Physics and Mathematical Physics, Adelaide University, Adelaide, South Australia 5005, Australia
(Received 17 January 2001; published 4 April 2002)

A recently proposed regularization-independent method is used for the first time to solve the renormalized fermion Schwinger-Dyson equation numerically in quenched four-dimensional QED. The Curtis-Pennington vertex is used to illustrate the technique and to facilitate comparison with previous calculations which used the alternative regularization schemes of modified ultraviolet cutoff and dimensional regularization. Our new results are in excellent numerical agreement with these, and so we can now conclude with confidence that there is no residual regularization dependence in these results. Moreover, from a computational point of view the regularization independent method has enormous advantages, since all integrals are absolutely convergent by construction, and so do not mix small and arbitrarily large momentum scales. We analytically predict power law behavior in the asymptotic region, which is confirmed numerically with high precision. The successful demonstration of this efficient new technique opens the way for studies of unquenched QED to be undertaken in the near future.

DOI: 10.1103/PhysRevD.65.085020 PACS number(s): 12.20.Ds, 11.10.Gh, 11.15.Tk

I. INTRODUCTION

The divergences inherent in quantum field theories have plagued physicists for years. The infinities are removed in a two-step process: first the divergences are controlled by a regulator, then the regulator is removed using the renormalization procedure to obtain finite, renormalization-independent physical quantities. Depending on the type of regulator introduced, different problems can occur. It is useful to discuss the difficulties that arise in the Schwinger-Dyson equations (SDE's) [1], since these are identical to the difficulties encountered in perturbation theory and because we will be using them as a tool to study nonperturbative QED. In the literature, SDE's in quenched four-dimensional QED (QED_4) are commonly studied by using the ultraviolet cutoff regularization scheme [2]. One difficulty faced is that the use of an ultraviolet (UV) cutoff Λ to regulate the integration will in general lead to an explicit violation of gauge covariance [3]. Because this regularization scheme does not respect translation invariance in the loop-momentum integration, it will lead to an explicit gauge-covariant violating contribution in the result, *even after* Λ is taken to infinity. More precisely, this violation of gauge invariance has been observed in quenched QED calculations employing the Curtis-Pennington (CP) [4] electron-photon vertex and may be traced back to a certain, logarithmically divergent, 4-dimensional momentum integral which vanishes because of rotational symmetry at all $\Lambda<\infty$, but leads to a finite contribution for $\Lambda\to\infty$. It is this discontinuous behavior as a function of Λ which complicates correct numerical renormalization with this regulator. Incorrect results will be obtained unless care is taken to identify and remove gauge-covariance violating terms [5–7]. In its favor, cutoff regularization is computationally economical and gives accurate answers after gauge-covariance violating terms are removed.

On the other hand, SDE studies implemented using a gauge-invariant regularization scheme, such as dimensional regularization [8], do not have such a problem. However a dynamical mass is generated for all coupling constants in $D<4$, instead of only above critical coupling in $D=4$ in cutoff regularization. In nonperturbative studies this scheme is computationally more demanding since a careful and time-consuming removal of the regulator must be performed, involving an extrapolation of many high-precision solutions for different ϵ to $\epsilon=0$. Additionally the accuracy of the results is, in practice, more limited because the integration range necessarily extends to infinity.

In this paper we will be employing for the first time the regulator-independent method recently proposed by Kızılersü *et al.* [9] to solve the renormalized fermion Schwinger-Dyson equation numerically in quenched QED_4. This method deals with renormalized quantities only, as the regulator is removed analytically. The dependence on the mass scale introduced by the regulator is traded for the momentum scale μ at which the theory is renormalized *before* performing any numerical calculations. In this way any regulator which does not violate gauge covariance (such as dimensional regularization or cutoff regularization modified as discussed above) can be used and the regulator removed analytically *before* any numerical calculations are begun. More importantly, from a numerical point of view, removal of the regulator means that no longer does one have to solve integral equations involving mass scales of vastly different orders of magnitude (and then, in addition, take a limit in which one of the scales goes to infinity). Rather, the important scales in the problem become scales of physical importance, e.g., the renormalized mass $m(\mu)$ and the renormalization scale μ at which this mass is defined. It is therefore to be expected that the dominant contributions to any integrands will be from a finite region of momenta. This feature is generic; i.e., it is independent of the particular vertex an-

*Email address: akiziler@physics.adelaide.edu.au
†Email address: tsizer@physics.adelaide.edu.au
‡Email address: awilliam@physics.adelaide.edu.au

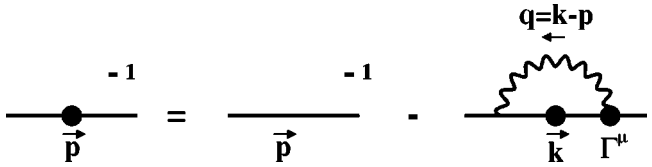

FIG. 1. The Schwinger-Dyson equation for the fermion propagator.

satz that one makes use of, and it remains a valid consideration for an arbitrary renormalizable field theory.

The regularization-independent approach is computationally very economical and very accurate, although one may lose direct contact with the bare theory. In particular, one cannot study dynamical chiral symmetry breaking in this approach by simply setting the bare mass $m_0=0$ and investigating at what value of coupling the dynamical fermion mass is generated. In Ref. [10], within quenched QED, a removal of the regulator was attempted in a manner which has some similarity to what we do here. As emphasized by Miransky (Refs. [11,12] as well as Chapter 10.7 of Ref. [13]), some care needs to be taken with the treatment of the bare mass while removing the regulator in order to avoid drawing incorrect conclusions about the presence or absence of dynamical chiral symmetry breaking in gauge theories.

In SDE studies of quenched QED_4 there is a critical coupling α_c, below which the fermion propagator is well behaved and the standard textbook renormalization procedure for renormalizing the nonperturbative propagator appears to be entirely adequate, e.g., see Refs. [1–5,7,8]. Atkinson *et al.* studied the transition through α_c within standard QED_4 using a bifurcation method [14]. It was found in the unrenormalized quenched theory that at critical coupling the solutions bifurcate and for $\alpha>\alpha_c$ the SDE's in the chiral limit admit both a trivial $M(p^2)=0$ solution and a solution $M(p^2)\neq 0$ with dynamical mass generation. For this reason, the transition is often referred to as a dynamical chiral symmetry breaking transition even though the conservation of the axial current is not explicitly demonstrated.

In the studies of renormalized quenched QED_4 in Refs. [1,2,5,7,8], the renormalization prescription that is used above critical coupling ($\alpha>\alpha_c$) is the same one that is used below critical coupling ($\alpha<\alpha_c$), i.e., the standard ''textbook'' definition. Above critical coupling in these studies the dynamically generated mass function becomes infinite as the regulator is removed in the chiral limit when the bare mass m_0 is held to zero as the regularization is removed. This does not happen in model studies of QCD [1] where a running coupling constant $\alpha_s(q^2)$ is used [1]. For finite renormalized solutions above critical coupling the unphysical behavior manifests itself as oscillations in the renormalized mass function $M(p^2)$ and this has been demonstrated with high numerical precision in the previously cited references. The interpretation of these results is that above critical coupling in quenched QED_4 a phase change has occurred, which is coincident with the onset of dynamical mass generation and inconsistent with the renormalized fermion being a physical excitation. We say that it is not a physical excitation in the sense that it does not have a Lehmann representation with a positive semidefinite spectral function in the timelike region. Hence, above critical coupling applying the ''textbook'' renormalization prescription of holding the renormalized fermion mass constant at some renormalization point as the regularization is removed may well be inappropriate. What should be done above critical coupling is that the physical excitations in the supercritical phase should be identified and it is the properties of these that should be held fixed as the regularization is removed. Since our purpose here is to establish and test a new technique for solving renormalized SDE's, we will restrict our consideration to the same supercritical renormalization scheme that was used in previous studies. This is done so that we can compare in detail to earlier published work and because the supercritical phase of quenched QED_4 is not yet well understood. Below critical coupling, we are still in the standard phase and the ''textbook'' renormalization applied here is quite appropriate.

For completeness and to put this work into context, we briefly summarize results of other studies of QED_4. Miransky [11–13] has studied the fermion self-energy in quenched QED in the ladder-approximation SDE in the Landau gauge. In this work there were two phases and this construction led to the conclusion of a nontrivial continuum limit of QED. Miransky interpreted the critical coupling α_c as an ultraviolet stable fixed point and decreased the bare coupling e_0 with cutoff in such a way that as the ultraviolet cutoff is removed the mass function $M(p^2)$ remains finite and no oscillations occur. There have been a number of other attempts to construct microscopic models of dynamical chiral symmetry breaking [15–18]. Holdom [15] questioned whether Miransky's method of renormalization represented a true renormalization-group flow. Bardeen *et al.* [16] emphasized that the strong coupling phase of QED may render 4-Fermi operators relevant; hence in this phase, we should be studying the gauged Nambu–Jona-Lasinio (NJL) model rather than QED in isolation. The vacuum polarization effect in model SDE studies is considered in Refs. [17–20] and it was concluded that there was a chiral phase transition that led to the triviality of QED [18]. Azcoiti *et al.* [21–23] used a combination of lattice simulations and mean-field approximation and found qualitative agreement with the work of Miransky and the conclusion that QED was nontrivial. Another nonperturbative tool, the nonperturbative renormalization group, was used in other studies [24] where it was concluded the QED was a trivial theory.

The only first-principles studies of nonperturbative QED are those based on lattice gauge theory. There have been a variety of lattice-based studies of QED [25–34]. It appears that recently these lattice studies are approaching agreement [29,34] that standard textbook (i.e., unquenched, noncompact) QED_4 is a trivial theory. These results support Landau's conjecture that in the continuum limit QED interactions are completely screened and the (renormalized) fine structure constant vanishes. It has been argued that the Landau pole problem of QED_4 is resolved since the region of parameter space where this occurs is unavailable to the theory because of dynamical chiral symmetry breaking [34]. It was noted that Kim *et al.* [29] did not find numerical support for the work of Azcoiti *et al.* [21–23].

In this work we limit ourselves to standard textbook [35] renormalization in the quenched theory, where the coupling is not renormalized and is independent of the cutoff, even above critical coupling. Our long-term goal is to simultaneously solve the fermion and photon propagator SDE's with a well-constrained ansatz for the fermion-photon vertex. In these future studies we hope to establish whether or not QED is trivial and/or whether additional four-Fermi interactions must be included. We compare our new regularization-free method, with previous numerical analyses of renormalized quenched CP QED by the current authors and their collaborators [2,5,7,9]. The application of textbook renormalization immediately leads to the fact that in quenched QED there is no renormalization of the photon propagator (i.e., $Z_3=1$ in that case) and hence, due to the Ward-Takahashi identity which ensures that $Z_1=Z_2$, there is no renormalization of the coupling constant.

In Sec. II we formulate the regularization-independent method for renormalized SDE for quenched QED in 4 dimensions with an arbitrary covariant gauge. Section III discusses the large momentum behavior of the fermion propagator and gives its analytical form. We go on to solve SDE's numerically in Euclidean space for the fermion wave-function renormalization function and the mass function employing the CP vertex. The integration range in these equations is taken to infinity analytically and subsequently evaluated using a combination of numerical and analytic results. We do this extrapolation to infinity to facilitate comparison with previous results at very high momentum scales and to compare these results with their asymptotic forms. We demonstrate numerically to high precision the agreement between the regularization independent approach and the modified cutoff and dimensional regularization schemes. Finally, in Sec. IV we summarize our results and conclude.

II. REGULARIZATION-FREE FORMALISM IN QUENCHED QED$_4$

The renormalized Schwinger-Dyson equation for the electron propagator (Fig. 1) can be formulated as

$$\begin{aligned} S^{-1}(\mu;p) &= Z_2(\mu)S^{0-1}(p) \\ &\quad - iZ_1(\mu)e_0^2\int \frac{d^dk}{(2\pi)^d}\Gamma^\alpha(\mu;p,k) \\ &\quad \times S(\mu;k)\gamma^\beta D^0_{\alpha\beta}(\mu;q) \\ &\equiv Z_2(\mu)S^{0-1}(p) - iZ_1(\mu)\overline{\Sigma}(p). \end{aligned} \tag{2.1}$$

Here $Z_1(\mu)$ and $Z_2(\mu)$ are the vertex and fermion wave-function renormalization constants respectively. These renormalization constants relate the regularized but unrenormalized (i.e. *bare*) and renormalized propagator and vertex by

$$\Gamma_\mu(k,p;\mu)=Z_1(\mu,\Lambda)\Gamma^{\rm bare}_\mu(k,p;\Lambda), \tag{2.2}$$

$$S(p;\mu)=Z_2^{-1}(\mu,\Lambda)S^{\rm bare}(p;\Lambda). \tag{2.3}$$

In quenched QED, there is no renormalization of the electron charge ($e_0^2=e_\mu^2=4\pi\alpha$) and the appropriate photon propagator is simply the tree-level form

$$D^0_{\alpha\beta}(q)=-\frac{1}{q^2}\left[\left(g_{\alpha\beta}-\frac{q_\alpha q_\beta}{q^2}\right)+\xi\frac{q_\alpha q_\beta}{q^2}\right], \tag{2.4}$$

where ξ is the covariant gauge parameter. We use $S(\mu;p)$ to denote the full fermion propagator renormalized at the momentum scale μ. It can be expressed in terms of two scalar functions $Z(\mu^2;p^2)$, the fermion wave-function renormalization function, and $M(p^2)$, the mass function, by

$$S(\mu;p)=\frac{Z(\mu^2;p^2)}{\not p - M(p^2)}. \tag{2.5}$$

Note that $S^0(p)\equiv 1/(\not p - m_0)$ is the tree-level fermion propagator (i.e., the bare fermion propagator in the absence of interactions). The full (proper) renormalized fermion-photon vertex is $\Gamma_\mu(\mu;k,p)$. Multiplying the fermion SDE Eq. (2.1) by $\not p$ and I and taking their respective spinor traces, we can separate the fermion self-energy $\overline{\Sigma}(p^2)$ into Dirac odd, $\overline{\Sigma}_d(p^2)$, and Dirac even, $\overline{\Sigma}_s(p^2)$, parts; i.e. $\overline{\Sigma}(p)=\not p\overline{\Sigma}_d(p^2)+\overline{\Sigma}_s(p^2)$; then we perform Wick rotation to the Euclidean space. This gives

$$Z^{-1}(\mu^2;p^2)=Z_2(\mu)-Z_1(\mu)\overline{\Sigma}_d(p^2), \tag{2.6}$$

$$M(p^2)Z^{-1}(\mu^2;p^2)=Z_2(\mu)m_0+Z_1(\mu)\overline{\Sigma}_s(p^2), \tag{2.7}$$

and these self-energies make use of any regularization scheme that does not violate gauge covariance. Here, the bar over these quantities indicates that we have explicitly separated out the renormalization constants $Z_i(\mu)$; note that for notational brevity we do not indicate the implicit dependence on μ^2 of $\overline{\Sigma}_{d,s}(p^2)$ through the function $Z(\mu^2;p^2)$.

Because of the Ward-Takahashi identity, which must be satisfied by any acceptable vertex ansatz for $\Gamma_\mu(\mu;k,p)$ and any acceptable renormalization scheme, one has $Z_1(\mu)=Z_2(\mu)$. Making use of this fact, Eqs. (2.6) and (2.7) can be rearranged as

$$Z_2^{-1}(\mu)=Z(\mu^2;p^2)-Z(\mu^2;p^2)\overline{\Sigma}_d(p^2), \tag{2.8}$$

$$M(p^2)=m_0+[M(p^2)\overline{\Sigma}_d(p^2)+\overline{\Sigma}_s(p^2)]. \tag{2.9}$$

In order to avoid cumbersome notation, we have not explicitly indicated functional dependence on the regulator in Eqs. (2.1)–(2.9) but it should be understood. The renormalization constants $Z_{1,2}(\mu)$ and the bare fermion mass m_0 are regulator dependent in the above equations. As one removes the regulator, the integrals on the right hand side of Eq. (2.1), and hence $\overline{\Sigma}_d(p^2)$ and $\overline{\Sigma}_s(p^2)$, diverge logarithmically. It is the defining feature of a renormalizable field theory that these divergences may be absorbed into the constants $Z_{1,2}(\mu)$ and into the bare mass m_0, rendering finite, regularization-independent limits for $Z(\mu^2;p^2)$ and $M(p^2)$.

However, we can make use of the p^2 independence of $Z_{1,2}(\mu)$ and m_0 in order to eliminate these constants from the above equations. The renormalization conditions for the fermion wave-function renormalization function and the mass function are

$$Z(\mu^2;\mu^2)=1 \quad \text{and} \quad M(\mu^2)\equiv m(\mu). \tag{2.10}$$

Note that $m(\mu)$ should not be confused with an explicit chiral symmetry breaking mass such as the current quark mass in QCD. Even in the chiral limit where the bare mass $m_0=0$, above critical coupling we can have dynamical mass generation and hence our $m(\mu)\neq 0$. Evaluating Eqs. (2.8) and (2.9) at a second momentum which we take to be $p^2=\mu^2$ and taking the difference one obtains the central equations that we solve here:

$$\begin{aligned} Z(\mu^2;p^2)&=1+Z(\mu^2;p^2)\overline{\Sigma}_d(p^2)-\overline{\Sigma}_d(\mu^2),\\ M(p^2)&=m(\mu)+[M(p^2)\overline{\Sigma}_d(p^2)+\overline{\Sigma}_s(p^2)]\\ &\quad-[m(\mu)\overline{\Sigma}_d(\mu^2)+\overline{\Sigma}_s(\mu^2)]. \end{aligned} \tag{2.11}$$

As the left-hand sides of these equations must be finite as the regulator is removed, then the right-hand side (RHS) must be also, even though the individual terms on the RHS may *separately* diverge.

These renormalized equations Eq. (2.11) with the regulator removed provide a starting point for nonperturbative investigations which have significant advantages over the usual treatment found in the literature [2–8]. In the following section we shall illustrate this approach by turning to the example of quenched QED with the Curtis-Pennington vertex.

III. QUENCHED QED WITH THE CURTIS-PENNINGTON VERTEX

In this section we use the regulator-independent method for solving the renormalized SDE in Eq. (2.11) in an arbitrary covariant gauge. As usual we write the full vertex as a sum of the Ball-Chiu vertex [36] (longitudinal part satisfying the Ward-Takahashi identity) and the Curtis-Pennington term [4] (the transverse part satisfying multiplicative renormalizability of the fermion propagator),

$$\begin{aligned} \Gamma^\mu(\mu;k,p)&=\Gamma^\mu_{BC}(\mu;k,p)+\tau_6(\mu;k,p)\\ &\quad\times[\gamma^\mu(p^2-k^2)+(p+k)^\mu(\not{k}-\not{p})], \end{aligned} \tag{3.1}$$

where $\Gamma^\mu_{BC}(\mu;k,p)$ and $\tau_6(\mu;k,p)$ are given in Appendix A. After performing the angular integration, Eq. (2.11) can be written as

$$\begin{aligned} Z(\mu^2;p^2)&=1-\frac{\alpha\xi}{4\pi}\int_{p^2}^{\mu^2}dk^2\frac{1}{[k^2+M^2(k^2)]}Z(\mu^2;k^2)\\ &\quad+\frac{\alpha}{4\pi}\int_0^\infty\frac{dk^2}{[k^2+M^2(k^2)]}\\ &\quad\times[Z(\mu^2;p^2)I(k^2,p^2)-I(k^2,\mu^2)], \end{aligned} \tag{3.2}$$

$$\begin{aligned} M(p^2)&=m(\mu)+\frac{\alpha}{4\pi}\int_0^\infty\frac{dk^2}{[k^2+M^2(k^2)]}\\ &\quad\times[J(k^2,p^2)-J(k^2,\mu^2)+M(p^2)I(k^2,p^2)\\ &\quad-m(\mu)I(k^2,\mu^2)], \end{aligned} \tag{3.3}$$

where the kernel functions $I(p^2,k^2)$ and $J(p^2,k^2)$ are also given in Appendix A. The kernels have the same form as Ref. [14] except that the gauge-covariance violating term has been removed, since it does not survive the four-dimensional momentum integration in the absence of a cutoff. This term does not vanish if the angular integral is done first with the radial integral taken to infinity afterward, which is why it must be removed by hand in the cutoff approach.

The above equations are finite as can be seen by analysis of the large momentum limits of the integrands for Z and M, which behave asymptotically as $(k^2)^{-n}$ and $(k^2)^{-r}$, respectively, where $n,r>1$. The equation for the wave-function renormalization function Eq. (3.2) is the same as Eq. (10) in Ref. [10]; however our treatment of the mass function differs from theirs.

A. Asymptotic limits of the solutions

In this subsection we solve Eqs. (3.2) and (3.3) analytically for momenta p^2 much larger than $M^2(p^2)$ (the asymptotic region) by linearizing them for finite mass, in a manner similar to that used by Atkinson *et al.* [14] for the chirally symmetric theory (i.e. $m_0=0$). It is convenient to *temporarily* take the renormalization point μ to also be very large, removing this constraint once our derivation is complete. When p^2 and μ^2 are in the asymptotic region k^2 is necessarily also much greater than $M^2(k^2)$; therefore expanding in powers of $M^2(k^2)/k^2$ and keeping at most linear terms in $M(k^2)$, the kernel functions take their asymptotic forms $I(p^2,k^2)\to 0$ and $J(p^2,k^2)\to k^2J'(p^2,k^2)$, where $J'(k^2;p^2)$ is defined in Appendix A. Hence when p^2 and μ^2 are both in the asymptotic region, we obtain

$$Z(\mu^2;p^2)=1-\frac{\alpha\xi}{4\pi}\int_{p^2}^{\mu^2}\frac{dk^2}{k^2}Z(\mu^2;k^2), \tag{3.4}$$

$$\begin{aligned} M(p^2)&=m(\mu)+\frac{\alpha}{4\pi}\int_0^\infty dk^2[J'(k^2,p^2)\\ &\quad-J'(k^2,\mu^2)]. \end{aligned} \tag{3.5}$$

These linearized equations admit power law solutions.

The solution of this asymptotic form of the Z equation is easily seen to be [3]

$$Z(\mu^2;p^2)=\left(\frac{p^2}{\mu^2}\right)^\nu \quad \text{with} \quad \nu=\frac{\alpha\xi}{4\pi}, \tag{3.6}$$

which differs from Ref. [14] due to the absence of the gauge covariance violating term. We thus obtain for p^2 and p'^2 both large that

$$\frac{Z(\mu^2;p^2)}{Z(\mu^2;p'^2)}=\left(\frac{p^2}{p'^2}\right)^{\nu} \quad \text{with} \quad \nu=\frac{\alpha\xi}{4\pi}, \tag{3.7}$$

which is valid for an *arbitrary* renormalization point μ since the ratio is by definition renormalization-point independent. It then follows for large p^2 and any arbitrary μ^2 that

$$Z(\mu^2;p^2)=C_\mu\left(\frac{p^2}{\mu^2}\right)^{\nu} \quad \text{with} \quad \nu=\frac{\alpha\xi}{4\pi}, \tag{3.8}$$

for some appropriate C_μ such that $C_\mu\to 1$ as μ^2 enters the asymptotic region.

We shall see that power law solutions of the M equation occur in two regimes, depending on the value of α. Those with a real exponent can be identified with the subcritical regime, where α is less than its critical value α_c which marks the onset of dynamical mass generation. Those with complex exponent correspond to oscillating solutions which correspond to the supercritical regime where $\alpha>\alpha_c$. We examine these two cases separately in what follows.

1. Subcritical asymptotic solution

Where, as before, μ^2 and p^2 are understood to be chosen much greater than all other mass scales, we try a solution of Eq. (3.5) of the form

$$M(p^2)=m(\mu)\left(\frac{p^2}{\mu^2}\right)^{-s}, \quad s\in R. \tag{3.9}$$

Solving for s, we find

$$\frac{3\nu}{2\xi}\left[2\pi\cot s\pi-\pi\cot\nu\pi+3\pi\cot(\nu-s)\pi+\frac{2}{(1-s)}+\frac{1}{(\nu+1)}+\frac{1}{\nu}-\frac{3}{(\nu-s)}-\frac{1}{(\nu-s+1)}\right]+\frac{s-1}{\nu-s+1}=0. \tag{3.10}$$

This equation is the same as in Ref. [14], but in contrast to the unrenormalized equation examined in that paper, this power ansatz is valid for the renormalized equation that we have here whether or not the bare mass m_0 is zero. We can again form a ratio, i.e., provided p^2 and p'^2 are much larger than all other mass scales, we have

$$\frac{M(p^2)}{M(p'^2)}=\left(\frac{p^2}{p'^2}\right)^{-s}, \quad s\in R. \tag{3.11}$$

Both Eqs. (3.10) and (3.11) are manifestly renormalization-point independent and so are valid for an arbitrary choice of renormalization point μ. It then follows that for large p^2 and any arbitrary μ^2 that

$$M(p^2)=D_\mu\left(\frac{p^2}{\mu^2}\right)^{-s}, \quad s,D_\mu\in R \tag{3.12}$$

for some appropriate D_μ. We see that $D_\mu/(\mu^2)^{-s}$ is a renormalization-point independent constant and that we must have $D_\mu\to m(\mu)$ as μ^2 moves into the asymptotic region.

There is in fact more than one real solution to s in Eq. (3.10) (see also Ref. [14]), e.g., in Landau gauge there are two. However, only one of these matches smoothly onto the perturbative solution, and hence is the relevant solution. The other solutions appear as a spurious by-product of the linearized approximation in Eq. (3.5). [Solutions that do not match smoothly onto perturbation theory can arise in Eq. (3.5) if the integrals diverge as $1/\alpha$, due to infrared divergences; this cannot occur in Eq. (3.3) because of the regulating mass in the denominator.] Since s is real there are no oscillations in the mass function. These solutions, $M(p^2\neq 0)$, in the subcritical region are explicit chiral symmetry breaking solutions.

2. Supercritical asymptotic solution

In the case where s is complex, the (real) mass function is a superposition of powers of s and its complex conjugate. For large p^2 and arbitrary μ^2 we have as the counterpart to Eq. (3.12)

$$M(p^2)=\frac{1}{2}D_\mu\left(\frac{p^2}{\mu^2}\right)^{-s}+\frac{1}{2}D_\mu^*\left(\frac{p^2}{\mu^2}\right)^{-s^*}, \quad s,D_\mu\in C, \tag{3.13}$$

where D_μ is some appropriate complex constant, and

$$\frac{1}{2}(D_\mu+D_\mu^*)=\mathrm{Re}(D_\mu)\to m(\mu) \tag{3.14}$$

as μ^2 enters the asymptotic region. Here s and s^* are complex conjugate solutions to Eq. (3.10) and the combination results in a mass function that oscillates. This oscillatory behavior is more transparent if we write Eq. (3.13) as

$$M(p^2)=\left(\frac{p^2}{\mu^2}\right)^{-\mathrm{Re}(s)}\{\mathrm{Re}(D_\mu)\cos[\mathrm{Im}(s)\log(p^2/\mu^2)]+\mathrm{Im}(D_\mu)\sin[\mathrm{Im}(s)\log(p^2/\mu^2)]\} \tag{3.15}$$

which has the form of a phase-shifted cosine function periodic in $\log(p^2/\mu^2)$, with a period of $2\pi/\mathrm{Im}(s)$, modulated by an exponentially decaying envelope of $(p^2/\mu^2)^{-\mathrm{Re}(s)}$. The oscillations are an indication of a new phase in quenched QED employing the CP vertex at sufficiently strong coupling $\alpha>\alpha_c$.

B. Numerical solutions

In the regularization-independent approach, the equations are constructed so as to remove all infinities from the outset and so the UV region of the integral is not a crucial limiting factor. Moreover, establishing exact asymptotic forms of the wave-function renormalization and mass functions in the previous subsection makes it possible to analytically integrate Eqs. (3.2) and (3.3) from the highest grid point to in-

finity. We denote this highest grid point, where the asymptotic analytic forms are matched onto the numerical results, as the "matching point" k_m^2. For $p^2 \geqslant k_m^2$, we use the analytic forms, while for $p^2 < k_m^2$ we can rewrite Eqs. (3.2) and (3.3) as

$$Z(\mu^2;p^2) \equiv 1 - \frac{\alpha\xi}{4\pi}\int_{p^2}^{\mu^2} dk^2 \frac{1}{[k^2+M^2(k^2)]} Z(\mu^2;k^2) + \frac{\alpha}{4\pi}\int_0^{k_m^2} \frac{dk^2}{[k^2+M^2(k^2)]} \times [Z(\mu^2;p^2)I(k^2,p^2) - I(k^2,\mu^2)] + Z_{\text{high}}(\mu^2;k_m^2,p^2), \tag{3.16}$$

$$M(p^2) \equiv m(\mu) + \frac{\alpha}{4\pi}\int_0^{k_m^2} \frac{dk^2}{[k^2+M^2(k^2)]} \times [J(k^2,p^2) - J(k^2,\mu^2) + M(p^2)I(k^2,p^2) - m(\mu)I(k^2,\mu^2)] + M_{\text{high}}(\mu^2;k_m^2,p^2), \tag{3.17}$$

where the matching point, k_m^2, is chosen sufficiently large that the asymptotic formulas are valid $[k_m^2 \gg M^2(k_m^2)]$. These equations serve as definitions of the analytic forms that we need to evaluate, i.e., $Z_{\text{high}}(\mu^2;k_m^2,p^2)$ and $M_{\text{high}}(\mu^2;k_m^2,p^2)$ are defined as the contributions arising from integrating from k_m^2 to infinity for Eqs. (3.16) and (3.17) respectively. The analytic forms for Z_{high} and M_{high} and their derivations are given in Appendix B. By calculating $Z(\mu^2;p^2)$ and $M(p^2)$ in this way we can achieve very high accuracy in the UV region.

Equations (3.16) and (3.17) have been solved numerically in Euclidean space for $Z(\mu^2;p^2)$ and $M(p^2)$ with a variety of gauges ξ, renormalization points μ^2, and renormalized masses $m(\mu)$ for the couplings $\alpha = 0.6$ (subcritical) and $\alpha = 1.5$ (supercritical). Each solution was iterated from an initial guess until $Z(\mu^2;p^2)$ and $M(p^2)$ converge; our convergence criterion is that the change in successive solutions is less than one part in 10^8 at each momentum point. At every iteration the data are refitted to the asymptotic analytic forms of $Z(\mu^2;p^2)$ and $M(p^2)$.

We have found, in line with the above discussion, that the regularization-independent method allows us to extend solutions for momenta up to 10^{65} as opposed to solutions obtained from cutoff regularization where numerical round-off error meant that the momenta in our solutions could typically not exceed $\mathcal{O}(10^{18})$ [2,5,7]. We also verified that our solutions do not change when we vary the location of the point k_m where the matching of our numerical and analytical solutions is carried out.

In Figs. 2 and 3, we show typical solutions, using regularization independent regularization, of the fermion wavefunction renormalization and mass functions for subcritical ($\alpha = 0.6$) and supercritical ($\alpha = 1.5$) cases respectively. Also shown are corresponding solutions based on the theoretical

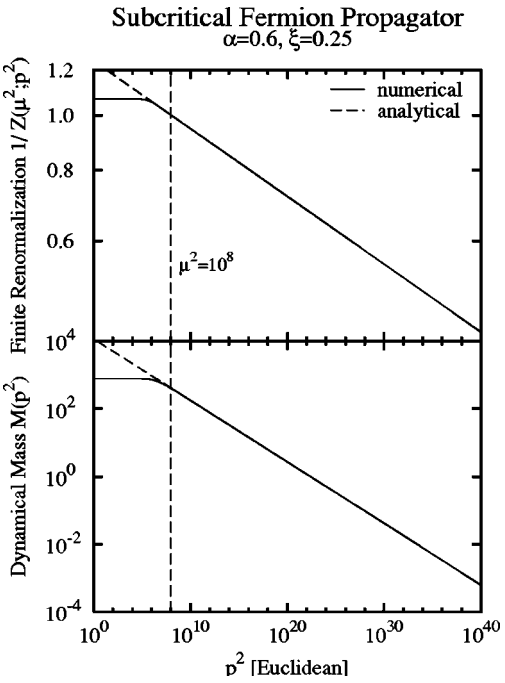

FIG. 2. Comparison of the numerical solution for the finite renormalization $1/Z(\mu^2;p^2)$ and the mass function $M(p^2)$ (solid lines) and their predicted asymptotic behavior with matching scales (dashed lines) from Eqs. (3.8) and (3.12) for the subcritical coupling $\alpha = 0.6$. The example solution was for a renormalized mass $m(\mu) = 400$ (arbitrary units), renormalization point $\mu^2 = 10^8$ and gauge parameter $\xi = 0.25$.

asymptotic powers with fitted scales. The log-log nature of the figures emphasizes the UV behavior of the propagator. One can see there is excellent agreement in the region $p^2 \gg M^2(p^2)$. To emphasize this point we present the theoretical and numerically calculated powers for these two solutions in Table I.

In summary, our knowledge of the exact forms of $Z(\mu^2;p^2)$ and $M(p^2)$ in the asymptotic region saves us from the need to extend our numerical solutions far into the ultraviolet. Therefore Eqs. (3.16) and (3.17) are solved numerically up to the matching point (k_m^2) in the UV, whereafter the analytical solution joins smoothly to the numerical one. The fitting parameters $[C_\mu, \text{Re}(D_\mu), \text{Im}(D_\mu), \text{Re}(s), \text{Im}(s), \nu]$ for the analytic continuation are recalculated after each iteration.

C. Comparison of regularization schemes

We can now compare numerical solutions from the regularization-independent approach to those from cutoff regularization with the gauge-covariance modification [2,5,7] and those from dimensional regularization [8]. In cutoff regularization the fermion self-energies are integrated on a logarithmically spaced grid in k^2 momentum up to the highest (cutoff) momentum Λ^2. Additionally, in dimensional regularization, an estimate is made of the contribution to the integral from the highest grid point to infinity. In both the modified cutoff and the dimensional regularization studies subtractive renormalization is performed numerically for the regularized (but otherwise divergent) fermion self-energies.

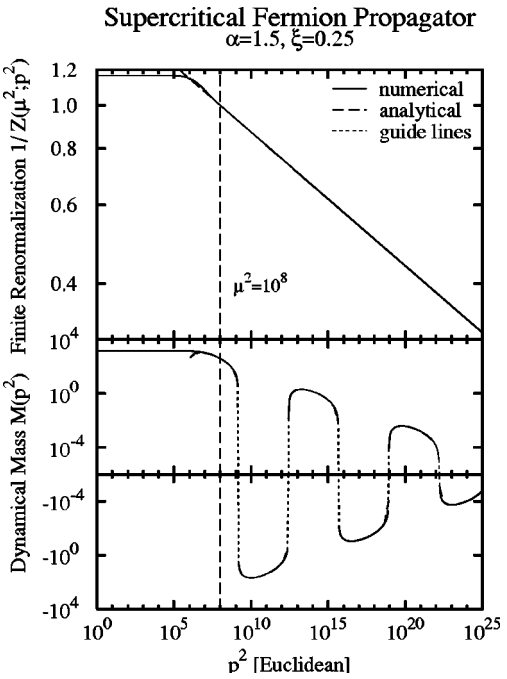

FIG. 3. Comparison of the numerical solution for the finite renormalization $1/Z(\mu^2;p^2)$ and the mass function $M(p^2)$ (solid lines) and their predicted asymptotic behavior with matching scales (dashed lines) from Eqs. (3.8) and (3.13) for the supercritical coupling $\alpha=1.5$. The example solution was for a renormalized mass $m(\mu)=400$ (arbitrary units), renormalization point $\mu^2=10^8$ and gauge parameter $\xi=0.25$. The ''guidelines'' are added simply to guide the eye between data points on this logarithmic plot.

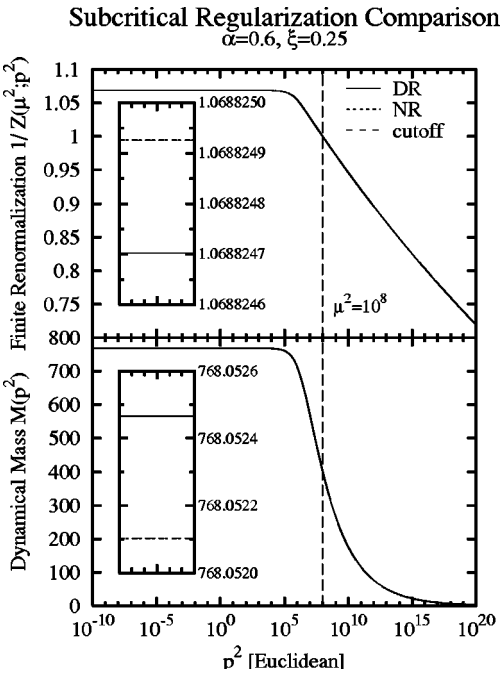

FIG. 4. The finite renormalization $1/Z(\mu^2;p^2)$ and dynamical mass $M(p^2)$ for the solution of the fermion SDE for subcritical coupling $\alpha=0.6$ and gauge parameter $\xi=0.25$ found from the regularization-independent (NR) method compared with solutions using the modified UV cutoff regulator and dimensional regularization. The dimensional regularization (DR) solution shown is the result of extrapolating various finite ϵ solutions at scale 10^3 to $\epsilon=0$ using a fit cubic in ϵ at each momentum point. All solutions have renormalized mass $m(\mu)=400$ (in arbitrary units) at the renormalization point $\mu^2=10^8$. The small variation between the three regularization schemes is entirely attributable to limitations achievable in numerical precision.

For the modified UV cutoff regularization approach it was necessary to perform the calculation at several values of Λ and in principle perform a $\Lambda\rightarrow\infty$ extrapolation. In practice it was found that it was sufficient simply to ensure that Λ was chosen large enough. For the dimensional regularization approach it was necessary to calculate solutions at high accuracy for very many values of ϵ and then carefully extrapolate ϵ to 0. Numerical limitations made it difficult to obtain solutions at very small ϵ, which in turn limits the achievable accuracy of the $\epsilon\rightarrow 0$ extrapolation.

In Figs. 4 and 5, we compare these three regularization methods for subcritical ($\alpha=0.6$) and supercritical ($\alpha=1.5$) cases respectively, with the standard parameter choice of $\xi=0.25, \mu^2=10^8, m(\mu)=400$. One can see that the agreement between the regulator-independent (NR) and the modified cutoff and dimensionally regularized (DR) solutions is excellent. They are indistinguishable on the main figures: the insets in Figs. 4 and 5 have the same p^2 scale and reveal the remarkable agreement between them in the infrared region. In Tables II and III we quantify the relative differences achieved between the three regularization schemes at a variety of momentum values. The difference between the results is entirely attributable to the limitations achievable in numerical precision. We can now conclude with some confi-

TABLE I. This table compares the powers of the asymptotes of the finite renormalization and mass functions in Figs. 2 and 3, as determined analytically and by fitting the numerical solutions to a power law form.

Figure	Coupling	Determination	ν	Re(s)	Im(s)
2	$\alpha=0.6$	analytical	0.01193662073	−0.181667015	
		numerical	0.01193662073	−0.181666808	
3	$\alpha=1.5$	analytical	0.02984155182	−0.416012578	0.418128942
		numerical	0.02984155183	−0.416012521	0.418129001

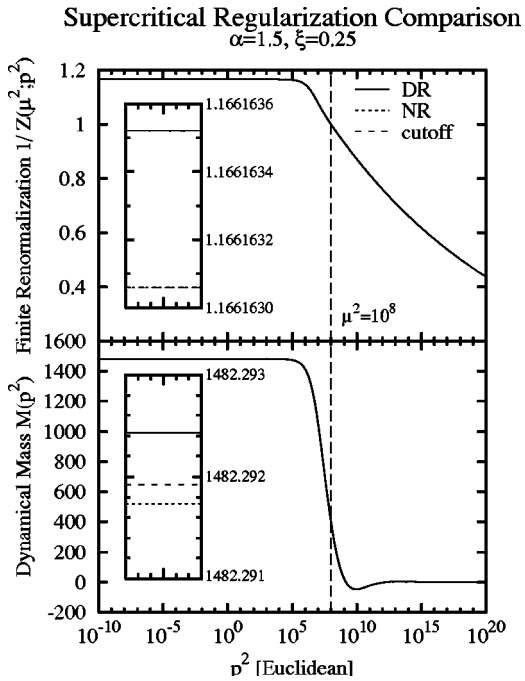

FIG. 5. The finite renormalization $1/Z(\mu^2;p^2)$ and dynamical mass $M(p^2)$ for the solution of the fermion SDE for supercritical coupling $\alpha=1.5$ and gauge parameter $\xi=0.25$ found from the regularization-independent (NR) method compared with solutions using the modified UV cutoff regulator and dimensional regularization. The dimensional regularization (DR) solution shown is the result of extrapolating various finite ϵ solutions at scale 10^3 to $\epsilon=0$ using a fit cubic in ϵ at each momentum point. All solutions have renormalized mass $m(\mu)=400$ (in arbitrary units) at the renormalization point $\mu^2=10^8$. The small variation between the three regularization schemes is entirely attributable to limitations achievable in numerical precision.

dence that the three regularization schemes give identical results for the renormalized solutions.

IV. CONCLUSIONS AND OUTLOOK

In this paper we have solved for the first time the Schwinger-Dyson equations for the fermion propagator in quenched QED_4 using the regularization-independent approach recently proposed in Ref. [9]. This has been done for the particular choice of the Curtis-Pennington transverse photon-fermion vertex, since this facilitates comparison with previous results which used the (gauge-covariance) modified UV cutoff and the dimensional regularization schemes. In addition, we have conformed with previous numerical studies [2,5–9], which used standard, ''textbook'' renormalization [35] below and above critical coupling. We have carried out precise calculations in these three approaches and have achieved excellent numerical agreement between them. This clearly demonstrates that we are able to achieve high-precision nonperturbative calculations of the renormalized fermion propagator that are free from any spurious errors which might arise from the regularization procedure itself.

We have derived and used the asymptotic analytic form of the solutions to obtain high accuracy even at extremely large momentum scales $[\mathcal{O}(10^{65})]$. The reason that this is possible now is because in the regularization-independent approach all momentum integrations are finite by construction; see Eq. (2.11). No bare mass or renormalization constants appear in this formulation, since they have been eliminated by combining and subracting renormalized quantities. The onset of the phase transition is signaled by the appearance of oscillations in the UV mass function. This is a well-studied phenomenon in quenched QED_4. We have derived the explicit analytical forms for the oscillations in the asymptotic region above critical coupling, including the period and decay envelope of these.

The importance of this regularization-independent approach lies in the fact that since all unregularized momentum integrations are finite from the outset, we do not have the mixing of small and arbitrarily large momentum scales in the intermediate stages of our numerical calculations. This means that we can achieve high accuracy for solutions in the low and medium momentum regime with great numerical economy. For *quenched* QED_4 it will be necessary to identify the true nature of the supercritical phase so that an appropriate renormalization procedure can be defined for this phase. This new approach will now permit numerically tractable studies of *unquenched* QED_4. These studies are now under way.

ACKNOWLEDGMENTS

This work was supported by the Australian Research Council. We thank Andreas Schreiber for numerous helpful discussions.

TABLE II. Relative differences achieved for the finite renormalization $1/Z(\mu^2;p^2)$ between the regularization-independent approach and the modified UV cutoff and dimensional regularization (for cubic and quartic fits) approaches. The differences are averages over all momentum points solved in each order of magnitude shown. The solution parameters are the same as those in Figs. 4 and 5.

	Regularization independent vs	$p^2=10^{-6}$	$p^2=10^{-2}$	$p^2=10^2$	$p^2=10^6$	$p^2=10^{10}$
$\alpha=0.6$	Modified cutoff	1.44×10^{-10}	1.45×10^{-10}	1.94×10^{-10}	5.35×10^{-8}	8.22×10^{-8}
	Dimensional regularization (cubic)	2.10×10^{-7}	2.10×10^{-7}	2.09×10^{-7}	9.05×10^{-8}	1.63×10^{-6}
	Dimensional regularization (quartic)	9.65×10^{-8}	9.64×10^{-8}	9.63×10^{-8}	6.11×10^{-8}	1.13×10^{-7}
$\alpha=1.5$	Modified cutoff	1.32×10^{-10}	1.73×10^{-10}	4.82×10^{-9}	4.97×10^{-8}	2.05×10^{-7}
	Dimensional regularization (cubic)	3.95×10^{-7}	3.95×10^{-7}	2.13×10^{-7}	2.23×10^{-7}	3.64×10^{-6}
	Dimensional regularization (quartic)	2.04×10^{-6}	2.04×10^{-6}	5.73×10^{-7}	1.27×10^{-7}	6.92×10^{-7}

TABLE III. This table shows the relative differences achieved for the mass function $M(p^2)$ between the regularization-independent approach and the modified UV cutoff and dimensional regularization approaches. The parameters are the same as those in Figs. 4 and 5.

	Regularization independent vs	$p^2=10^{-6}$	$p^2=10^{-2}$	$p^2=10^{2}$	$p^2=10^{6}$	$p^2=10^{10}$
$\alpha=0.6$	Modified cutoff	2.63×10^{-10}	2.63×10^{-10}	3.19×10^{-10}	3.51×10^{-7}	1.58×10^{-6}
	Dimensional regularization (cubic)	4.73×10^{-7}	4.73×10^{-7}	4.73×10^{-7}	4.52×10^{-7}	2.34×10^{-5}
	Dimensional regularization (quartic)	5.16×10^{-7}	5.16×10^{-7}	5.16×10^{-7}	9.88×10^{-7}	4.18×10^{-6}
$\alpha=1.5$	Modified cutoff	1.24×10^{-7}	1.24×10^{-7}	1.23×10^{-7}	2.57×10^{-7}	6.47×10^{-5}
	Dimensional regularization (cubic)	4.68×10^{-7}	4.68×10^{-7}	9.29×10^{-7}	1.08×10^{-6}	2.06×10^{-4}
	Dimensional regularization (quartic)	1.64×10^{-6}	1.64×10^{-6}	5.22×10^{-7}	4.26×10^{-7}	3.74×10^{-5}

APPENDIX A

The expressions mentioned in Sec. III are given below. The Ball-Chiu vertex [36] is

$$\Gamma^{\mu}_{BC}(\mu;k,p)=\frac{1}{2}\left(\frac{1}{Z(\mu^2;k^2)}+\frac{1}{Z(\mu^2;p^2)}\right)\gamma^{\mu}+\frac{(k+p)^{\mu}}{k^2-p^2}\left[\left(\frac{1}{Z(\mu^2;k^2)}-\frac{1}{Z(\mu^2;p^2)}\right)\frac{(\not{k}+\not{p})}{2}-\left(\frac{M(k^2)}{Z(\mu^2;k^2)}-\frac{M(p^2)}{Z(\mu^2;p^2)}\right)\right]. \tag{A1}$$

The coefficient function of the transverse vertex (Curtis-Pennington) [4] is

$$\tau_6(\mu;k,p)=-\frac{1}{2d}\left(\frac{1}{Z(\mu^2;k^2)}-\frac{1}{Z(\mu^2;p^2)}\right),$$

where

$$d=\frac{\{(k^2-p^2)^2+[M^2(k^2)+M^2(p^2)]^2\}}{(k^2+p^2)}. \tag{A2}$$

The constituents of the integrands in Eqs. (3.2) and (3.3) are the renormalization-point independent kernel functions:

$$I(k^2,p^2)=\frac{3}{2(k^2-p^2)}\left\{M(k^2)\left[M(k^2)-M(p^2)\frac{Z(\mu^2;k^2)}{Z(\mu^2;p^2)}\right]+\frac{1}{2}\frac{(k^2+p^2)[M^2(k^2)+M^2(p^2)]^2}{\{(k^2-p^2)^2+[M^2(k^2)+M^2(p^2)]^2\}}\left[1-\frac{Z(\mu^2;k^2)}{Z(\mu^2;p^2)}\right]\right\}\times\left(\frac{k^4}{p^4}\theta(p^2-k^2)+\theta(k^2-p^2)\right)+\xi\frac{Z(\mu^2;k^2)}{Z(\mu^2;p^2)}\frac{M(k^2)M(p^2)}{k^2}\left(\frac{k^4}{p^4}\theta(p^2-k^2)\right), \tag{A3}$$

$$J(k^2,p^2)=\frac{3}{2}M(k^2)\left\{1+\frac{Z(\mu^2;k^2)}{Z(\mu^2;p^2)}+\frac{(k^4-p^4)}{\{(k^2-p^2)^2+[M^2(k^2)+M^2(p^2)]^2\}}\left(1-\frac{Z(\mu^2;k^2)}{Z(\mu^2;p^2)}\right)\right\}\times\left(\frac{k^2}{p^2}\theta(p^2-k^2)+\theta(k^2-p^2)\right)-\frac{3}{2}p^2\frac{Z(\mu^2;k^2)}{Z(\mu^2;p^2)}\frac{[M(k^2)-M(p^2)]}{k^2-p^2}\left(\frac{k^4}{p^4}\theta(p^2-k^2)+\theta(k^2-p^2)\right)+\xi\frac{Z(\mu^2;k^2)}{Z(\mu^2;p^2)}M(k^2)\left(\frac{k^2}{p^2}\theta(p^2-k^2)\right). \tag{A4}$$

Linearizing Eqs. (A3) and (A4) in terms of the mass function yields

$$I(k^2,p^2)\xrightarrow[k^2,p^2\gg M^2]{}I'(k^2,p^2)\equiv 0,$$

$$J(k^2,p^2)\xrightarrow[k^2,p^2\gg M^2]{}k^2J'(k^2,p^2),$$

where

$$J'(k^2,p^2)=\xi\frac{1}{p^2}\frac{Z(\mu^2;k^2)}{Z(\mu^2;p^2)}M(k^2)\,\theta(p^2-k^2)$$
$$+\frac{3}{2}\left\{\frac{2M(k^2)}{(p^2-k^2)}\left[p^2\frac{Z(\mu^2;k^2)}{Z(\mu^2;p^2)}-k^2\right]\right.$$
$$\times\left[\frac{\theta(p^2-k^2)}{p^2}+\frac{\theta(k^2-p^2)}{k^2}\right]$$
$$\left.-\frac{Z(\mu^2;k^2)}{Z(\mu^2;p^2)}\frac{M(p^2)-M(k^2)}{(p^2-k^2)}\right.$$
$$\left.\times\left[\frac{k^2}{p^2}\theta(p^2-k^2)+\frac{p^2}{k^2}\theta(k^2-p^2)\right]\right\}. \quad \text{(A5)}$$

APPENDIX B

This appendix is devoted to the analytic calculation of the wave-function renormalization and mass functions in the asymptotic limit. The quantities that we need to evaluate are

$$Z_{\rm high}(\mu^2;k_m^2,p^2)\equiv\frac{\alpha}{4\pi}\int_{k_m^2}^{\infty}\frac{dk^2}{k^2+M^2(k^2)}$$
$$\times[Z(\mu^2;p^2)I(k^2,p^2)-I(k^2,\mu^2)],$$

$$M_{\rm high}(\mu^2;k_m^2,p^2)$$
$$\equiv\frac{\alpha}{4\pi}\int_{k_m^2}^{\infty}\frac{dk^2}{k^2+M^2(k^2)}[J(k^2,p^2)-J(k^2,\mu^2)$$
$$+M(p^2)I(k^2,p^2)-m(\mu)I(k^2,\mu^2)], \quad \text{(B1)}$$

where $I(k^2,p^2)$ and $J(k^2,p^2)$ are given in Appendix A. Provided k_m^2 is sufficiently large that $k_m^2\gg M^2(k_m^2)$, these quantities become

$$\int_{k_m^2}^{\infty}\frac{dk^2}{k^2+M^2(k^2)}I(k^2,p^2)$$
$$=\int_{k_m^2\gg M^2(k_m^2)}^{\infty}\frac{dk^2}{k^2}\left\{-\frac{3}{2}\frac{M(p^2)M(k^2)}{(k^2-p^2)}\frac{Z(\mu^2;k^2)}{Z(\mu^2;p^2)}\right.$$
$$\left.+\frac{3}{4}M^4(p^2)\frac{(p^2+k^2)}{(k^2-p^2)^3}\left(1-\frac{Z(\mu^2;k^2)}{Z(\mu^2;p^2)}\right)\right\},$$

$$\int_{k_m^2}^{\infty}\frac{dk^2}{k^2+M^2(k^2)}J(k^2,p^2)$$
$$=\int_{k_m^2\gg M^2(k_m^2)}^{\infty}\frac{dk^2}{k^2}\left\{3M(k^2)+3M(k^2)\frac{p^2}{(k^2-p^2)}\right.$$
$$\times\left(1-\frac{Z(\mu^2;k^2)}{Z(\mu^2;p^2)}\right)$$
$$\left.-\frac{3}{2}p^2\frac{Z(\mu^2;k^2)}{Z(\mu^2;p^2)}\frac{M(k^2)-M(p^2)}{(k^2-p^2)}\right\}. \quad \text{(B2)}$$

We have already shown for $k^2\gg M^2$ that the wave-function renormalization and the mass function have a power law behavior:

$$Z(\mu^2;k^2)=C_\mu\left(\frac{k^2}{\mu^2}\right)^{\nu},$$

$$M(k^2)=\frac{1}{2}D_\mu\left(\frac{k^2}{\mu^2}\right)^{-s}+\frac{1}{2}D_\mu^*\left(\frac{k^2}{\mu^2}\right)^{-s^*}. \quad \text{(B3)}$$

The results for $Z_{\rm high}$ and $M_{\rm high}$ for large k_m^2 and arbitrary $p^2,\mu^2<k_m^2$ can then be given in terms of hypergeometric functions:

$$Z_{\rm high}(\mu^2;k_m^2,p^2)=\frac{3\alpha}{16\pi}[Z(\mu^2;p^2)\tilde{I}(p^2)-\tilde{I}(\mu^2)],$$

$$M_{\rm high}(\mu^2;k_m^2,p^2)=\frac{3\alpha}{16\pi}[2\tilde{J}(p^2)-2\tilde{J}(\mu^2)$$
$$+M(p^2)\tilde{I}(p^2)-m(\mu)\tilde{I}(\mu^2)], \quad \text{(B4)}$$

with

$$\tilde{I}(p^2)=M^4(p^2)\left[\frac{p^2}{3(k_m^2)^3}F(3,3,4,p^2/k_m^2)+\frac{1}{2(k_m^2)^2}F(3,2,3,p^2/k_m^2)\right]$$
$$-\frac{M^4(p^2)}{Z(\mu^2;p^2)}\frac{C_\mu}{(\mu^2)^\nu}\left[\frac{1}{(3-\nu)}\frac{p^2}{(k_m^2)^{3-\nu}}F(3,3-\nu,4-\nu,p^2/k_m^2)+\frac{1}{(2-\nu)}\frac{1}{(k_m^2)^{2-\nu}}F(3,2-\nu,3-\nu,p^2/k_m^2)\right]$$
$$+\frac{M(p^2)}{Z(\mu^2;p^2)}\frac{C_\mu D_\mu}{(\mu^2)^{\nu-s}}\frac{(k_m^2)^{\nu-s-1}}{(\nu-s-1)}F(1,1-\nu+s,2-\nu+s,p^2/k_m^2)$$
$$+\frac{M(p^2)}{Z(\mu^2;p^2)}\frac{C_\mu D_\mu^*}{(\mu^2)^{\nu-s^*}}\frac{(k_m^2)^{\nu-s^*-1}}{(\nu-s^*-1)}F(1,1-\nu+s^*,2-\nu+s^*,p^2/k_m^2) \tag{B5}$$

and

$$\tilde{J}(p^2)=\frac{D_\mu}{(\mu^2)^{-s}}\frac{p^2}{(1+s)(k_m^2)^{s+1}}F(1,1+s,2+s,p^2/k_m^2)+\frac{D_\mu^*}{(\mu^2)^{-s^*}}\frac{p^2}{(1+s^*)(k_m^2)^{s^*+1}}F(1,1+s^*,2+s^*,p^2/k_m^2)$$
$$-\frac{3}{2}\frac{C_\mu D_\mu}{(\mu^2)^{\nu-s}Z(\mu^2;p^2)}\frac{p^2}{(1+s-\nu)(k_m^2)^{s-\nu+1}}F(1,1+s-\nu,2+s-\nu,p^2/k_m^2)$$
$$-\frac{3}{2}\frac{C_\mu D_\mu^*}{(\mu^2)^{\nu-s^*}Z(\mu^2;p^2)}\frac{p^2}{(1+s^*-\nu)(k_m^2)^{s^*-\nu+1}}F(1,1+s^*-\nu,2+s^*-\nu,p^2/k_m^2)$$
$$-\frac{C_\mu}{(\mu^2)^\nu}\frac{M(p^2)}{Z(\mu^2;p^2)}\frac{p^2}{(\nu-1)(k_m^2)^{1-\nu}}F(1,1-\nu,2-\nu,p^2/k_m^2). \tag{B6}$$

[1] C.D. Roberts and A.G. Williams, Prog. Part. Nucl. Phys. **33**, 477 (1997).

[2] F.T. Hawes and A.G. Williams, Phys. Rev. D **51**, 3081 (1995), and references therein.

[3] Z. Dong, H. Munczek, and C.D. Roberts, Phys. Lett. B **333**, 536 (1994).

[4] D.C. Curtis and M.R. Pennington, Phys. Rev. D **42**, 4165 (1990), and references therein.

[5] F.T. Hawes, A.G. Williams, and C.D. Roberts, Phys. Rev. D **54**, 5361 (1996).

[6] A. Kızılersü, T. Sizer, and A.G. Williams, Report No. ADP-99-43-T380, hep-ph/0001147.

[7] F.T. Hawes, T. Sizer, and A.G. Williams, Phys. Rev. D **55**, 3866 (1997).

[8] A.W. Schreiber, T. Sizer, and A.G. Williams, Phys. Rev. D **58**, 125014 (1998); V.P. Gusynin, A.W. Schreiber, T. Sizer, and A.G. Williams, *ibid.* **60**, 065007 (1999).

[9] A. Kızılersü, A.W. Schreiber, and A.G. Williams, Phys. Lett. B **499**, 261 (2001).

[10] D.C. Curtis and M.R. Pennington, Phys. Rev. D **46**, 2663 (1992).

[11] V.A. Miransky, Phys. Lett. **165B**, 401 (1985); Nuovo Cimento A **90**, 149 (1985); see also D. Atkinson and P.W. Johnson, Phys. Rev. D **35**, 1943 (1987).

[12] P.I. Fomin, V.P. Gusynin, V.A. Miransky, and Yu.A. Sitenko, Riv. Nuovo Cimento **6**, 1 (1983).

[13] V.A. Miransky, *Dynamical Symmetry Breaking in Quantum Field Theories* (World Scientific, Singapore, 1993).

[14] D. Atkinson *et al.*, Phys. Lett. B **329**, 117 (1994).

[15] B. Holdom, Phys. Rev. Lett. **62**, 997 (1989); **63**, 1889 (1989).

[16] W.A. Bardeen, C.N. Leung, and S.T. Love, Phys. Rev. Lett. **56**, 1230 (1986); C.N. Leung, S.T. Love, and W.A. Bardeen, Nucl. Phys. **B273**, 649 (1986); W.A. Bardeen, C.N. Leung, and S.T. Love, *ibid.* **B323**, 493 (1989); W.A. Bardeen, S.T. Love, and V.A. Miransky, Phys. Rev. D **42**, 3514 (1990).

[17] K.-I. Kondo, Y. Kikukawa, and H. Mino, Phys. Lett. B **220**, 270 (1989).

[18] K.-I. Kondo and H. Nakatani, Nucl. Phys. **B351**, 236 (1991); K.-I. Kondo, Int. J. Mod. Phys. A **6**, 5447 (1991); Nucl. Phys. **B351**, 259 (1991); Int. J. Mod. Phys. A **7**, 7239 (1992); K.-I. Kondo, H. Mino, and H. Nakatani, Mod. Phys. Lett. A **7**, 1509 (1992).

[19] V. Gusynin, Mod. Phys. Lett. A **5**, 133 (1990).

[20] J. Oliensis and P.W. Johnson, Phys. Rev. D **42**, 656 (1990).

[21] V. Azcoiti, G. DiCarlo, A. Gallante, A.F. Grillo, V. Laliena, and C.E. Piedrafita, Phys. Lett. B **355**, 270 (1995).

[22] V. Azcoiti, G. DiCarlo, and A.F. Grillo, Int. J. Mod. Phys. A **8**, 4235 (1993).

[23] V. Azcoiti, G. DiCarlo, A. Gallante, A.F. Grillo, V. Laliena, and C.E. Piedrafita, Phys. Lett. B **379**, 179 (1996).

[24] K.-I. Aoki, Int. J. Mod. Phys. B **4**, 1249 (2000).

[25] J.B. Kogut, E. Dagatto, and A. Kocic, Phys. Rev. Lett. **60**, 772 (1988).

[26] J.B. Kogut, E. Dagatto, and A. Kocic, Nucl. Phys. **B317**, 253 (1989).
[27] A. Kocic, J.B. Kogut, M.P. Lombardo, and K.C. Wang, Nucl. Phys. **B397**, 451 (1993).
[28] S.J. Hands, A. Kocic, J.B. Kogut, R.L. Renken, D.K. Sinclair, and K.C. Wang, Nucl. Phys. **B413**, 503 (1994).
[29] S. Kim, J.B. Kogut, and M.-P. Lombardo, Phys. Lett. B **502**, 345 (2001).
[30] P.E.L. Rakow, Nucl. Phys. **B356**, 27 (1991).
[31] M. Gockeler, R. Horsley, E. Laermann, P. Rakow, G. Schierholz, R. Sommer, and U.J. Wiese, Phys. Lett. B **251**, 567 (1990).
[32] M. Gockeler, R. Horsley, P. Rakow, G. Schierholz, and R. Sommer, Nucl. Phys. **B371**, 713 (1992).
[33] M. Gockeler, R. Horsley, V. Linke, P. Rakow, G. Schierholz, and H. Stuben, Phys. Rev. Lett. **80**, 4119 (1998).
[34] M. Gockeler, R. Horsley, V. Linke, P. Rakow, G. Schierholz, and H. Stuben, Nucl. Phys. B (Proc. Suppl.) **63**, 694 (1998).
[35] J.D. Bjorken and S.D. Drell, *Relativistic Quantum Fields* (McGraw-Hill, New York, 1965).
[36] J.S. Ball and T.W. Chiu, Phys. Rev. D **22**, 2512 (1980).